Annexin A6 improves anti-migratory and anti-invasive properties of tyrosine kinase inhibitors in EGFR overexpressing human squamous epithelial cells

Monira Hoque[1¶&], Yasmin A. Elmaghrabi[1¶], Meryem Köse[1#], Syed S. Beevi[1Δ], Jaimy Jose[1], Elsa Meneses-Salas[2], Patricia Blanco-Muñoz[2], James R.W. Conway[3,4x], Alexander Swarbrick[3,4], Paul Timpson[3,4], Francesc Tebar[2], Carlos Enrich[2], Carles Rentero[2*], Thomas Grewal[1*]

[1]School of Pharmacy, Faculty of Medicine and Health, University of Sydney, Sydney, NSW 2006, Australia.
[2]Departament de Biomedicina, Unitat de Biologia Cel·lular, Centre de Recerca Biomèdica CELLEX, IDIBAPS, Facultat de Medicina i Ciències de la Salut, Universitat de Barcelona, Spain.
[3]Cancer Research Program, Garvan Institute of Medical Research and Kinghorn Cancer Centre, Sydney, NSW 2010, Australia.
[4]St. Vincent's Clinical School, Faculty of Medicine, University of New South Wales Sydney, Sydney, NSW 2052, Australia.

[¶]These authors contributed equally to this work

[&]current address: Save Sight Institute, Sydney Medical School, University of Sydney, Sydney, NSW 2000, Australia.
[#]current address: PharmaCenter Bonn, Pharmaceutical Institute, Pharmaceutical Chemistry I, University of Bonn, An der Immenburg 4, D-53121 Bonn, Germany.
[Δ] current address: KIMS Foundation and Research Centre, KIMS Hospitals, 1-8-31/1, Minister Road, Secunderabad 500003, Telangana, India.
[x] current address: Turku Bioscience Centre, University of Turku and Åbo Akademi University, FI-20520 Turku, Finland.

*Corresponding authors:
Thomas Grewal, School of Pharmacy, Faculty of Medicine and Health, University of Sydney, Sydney, NSW 2006, Australia; Tel +612 9351 8496; Email thomas.grewal@sydney.edu.au
Carles Rentero, Departament de Biomedicina, Unitat de Biologia Cel·lular, Centre de Recerca Biomèdica CELLEX, IDIBAPS, Facultat de Medicina i Ciències de la Salut, Universitat de Barcelona, 08036 Barcelona, Spain. Tel. +34 227 5400 ext. 3358; Email carles.rentero@ub.edu

Running title: AnxA6 improves EGFR tyrosine kinase inhibitors

Abbreviations: Aki1, Akt kinase-interacting protein 1; Akt, protein kinase B; Anx, annexin; Ca^{2+}, calcium; EGF; epidermal growth factor; EGFR, epidermal growth factor receptor; Erk, extracellular signal-regulated kinase; MAPK, mitogen activated protein kinase; PKCα, protein kinase Cα; shRNA, short hairpin RNA; T, threonine; TK, tyrosine kinase; TKI, tyrosine kinase inhibitor; wt, wildtype; Y, tyrosine.

Keywords: Annexin A6, PKCα, EGFR, TKIs, A431 epithelial cells

Abstract

Annexin A6 (AnxA6), a member of the calcium (Ca^{2+}) and membrane binding annexins, is known to stabilize and establish the formation of multifactorial signaling complexes. At the plasma membrane, AnxA6 is a scaffold for protein kinase Cα (PKCα) and GTPase activating protein p120GAP to promote downregulation of epidermal growth factor receptor (EGFR) and Ras/mitogen activated protein kinase (MAPK) signaling. In human squamous A431 epithelial carcinoma cells, which overexpress EGFR, but lack endogenous AnxA6, restoration of AnxA6 expression (A431-A6) promotes PKCα-mediated threonine 654 (T654)-EGFR phosphorylation, which inhibits EGFR tyrosine kinase activity. This is associated with reduced A431-A6 cell growth, but also decreased migration and invasion in wound healing, matrigel and organotypic matrices. Here we show that A431-A6 cells display reduced EGFR activity *in vivo*, with xenograft analysis identifying increased pT654-EGFR levels, but reduced tyrosine EGFR phosphorylation compared to controls. In contrast, PKCα depletion in A431-A6 tumors is associated with strongly reduced pT654 EGFR levels, yet increased EGFR tyrosine phosphorylation and MAPK activity. Moreover, tyrosine kinase inhibitors (TKIs; gefitinib, erlotinib) more effectively inhibit cell viability, clonogenic growth, and wound healing of A431-A6 cells compared to controls. Likewise, the ability of AnxA6 to inhibit A431 motility and invasiveness strongly improve TKI efficacy in matrigel invasion assays. This correlates with a greatly reduced invasion of the surrounding matrix of TKI-treated A431-A6 when cultured in 3D-spheroids. Altogether these findings implicate that elevated AnxA6 scaffold levels contribute to improve TKI-mediated inhibition of growth and migration, but also invasive properties in EGFR overexpressing human squamous epithelial carcinoma.

Introduction

At the cell surface, growth factor receptors couple environmental cues with signaling cascades that regulate growth, motility and many other processes. Epidermal growth factor receptor (EGFR, ErbB1) is among the best-studied growth factor receptors, which upon ligand binding and dimerization, activates its tyrosine kinase (TK) domain. This is followed by tyrosine (Y) autophosphorylation and binding of adaptors, which then connect to downstream effector pathways [1-3].

To regain responsiveness for new inputs and prevent constitutive signaling and cell transformation, activated EGFR is rapidly downregulated. The cellular means to terminate EGFR signaling are multifaceted and the majority of activated EGFR is internalized and targeted to lysosomes for degradation [2-5]. Adding further complexity, recruitment of phosphotyrosine phosphatases dephosphorylate and inactivate EGFR at the cell surface and intracellular compartments [2-5]. In addition, at the plasma membrane protein kinase Cα (PKCα) phosphorylates EGFR at threonine 654 (T654), which inhibits EGFR TK activity and the associated mitogenic response [6, 7]. However, PKCα levels vary in EGFR-related cancers, with limited evidence on its contribution to influence oncogenic EGFR signaling [8, 9].

Aberrant activation of effector pathways due to EGFR overexpression or mutation contribute to more than 30% of human cancers [10-12]. This high incidence of EGFR-related cancers and its association with poor clinical prognosis paved the way to develop therapeutic interventions, including small molecule tyrosine kinase inhibitors (TKIs), such as gefitinib and erlotinib. Both TKIs have been approved to treat non-small cell lung cancers (NSCLC), where EGFR overexpression is commonly observed in squamous cell carcinomas, representing 20-30% of NSCLC (13, 14). TKIs have also shown therapeutic potential in squamous cell carcinoma of the head and neck (HNSCC), with the majority of those overexpressing EGFR (15, 16). However, primary or acquired resistance after therapy, but also poorly understood additional genetic alterations, contribute to variability in patient response, complicating predictions on the clinical effectiveness of TKIs targeting EGFR [12-14].

The presence or absence of scaffold proteins, which are known to recruit positive and negative regulators of the EGFR and its effectors to establish protein-protein interactions that modulate their signal output [14-16] further complicates efforts to foresee TKI efficacy. Hence, as the relative amounts of scaffolds can substantially influence the strength of EGFR signaling networks, this has potential to alter TKI efficacy. Indeed, aberrant expression of

cortactin is associated with resistance to gefitinib in head and neck squamous cell carcinoma [14]. Furthermore, silencing of the Akt kinase-interacting protein 1 (Aki1), a scaffold for the EGFR effector phosphoinositide 3-kinase, potentiates the growth inhibitory effect of new generation EGFR-TKIs in EGFR mutant lung cancer cells [17]. Also, up- or downregulation of scaffold proteins like caveolin and kinase suppressor of Ras alter sensitivity towards drugs targeting the EGFR or the mitogen activated protein kinase (MAPK) pathway in lung adenocarcinoma and other cancers [18-20].

In this context, we and others identified several members of the evolutionary conserved annexin protein family as scaffolds affecting the activity of EGFR signaling pathways [21-25]. This includes annexin A6 (AnxA6), which like other annexins, binds to phospholipids in a Ca^{2+}-dependent manner, enabling rapid translocation to the plasma membrane and endosomes [26-28]. In these locations, AnxA6 participates in signal complex formation, cytoskeleton re-arrangements, membrane organization and cholesterol transport [23-29]. We initially demonstrated that AnxA6 upregulation stabilized the assembly of the Ras-GTPase activating protein p120GAP with H-Ras to inhibit EGFR-induced Ras/MAPK signaling [30-32]. In addition, elevated AnxA6 levels increased membrane association of PKCα [33] and promoted PKCα-mediated EGFR inactivation in EGFR overexpressing A431, head and neck and breast cancer cell lines, thereby strongly reducing cell growth [34]. More recently we also established that upregulation of AnxA6 in A431 cells and other cell models correlated with reduced cell migration in wound healing and 3D-migration/invasion assays [35].

Based on these observations we hypothesized that AnxA6 expression levels in EGFR overexpressing squamous A431 epithelial cells may influence the efficacy of TKIs targeting EGFR. In this study, we demonstrate that AnxA6 also inhibits EGFR activity in A431 cells in a PKCα-dependent manner *in vivo*. Elevated AnxA6 levels in A431 cells more effectively enable gefitinib and erlotinib to inhibit cell growth and migration. Strikingly, TKI efficacy to inhibit A431 cell invasion in matrigel invasion assays and 3D-spheroids is strongly improved upon AnxA6 upregulation. The potential of the AnxA6 scaffold to alter TKI-mediated inhibition of growth and migration, but also invasive properties in squamous carcinoma cells with de-regulated EGFR expression is discussed.

Results

Annexin A6 inhibits EGFR activation in a PKCα-dependent manner in A431 cells

We first compared EGFR phosphorylation in A431wt, which express 1-3 x 10^6 EGFRs/cell, but lack endogenous AnxA6 [30, 32, 36], and A431 stably expressing AnxA6 (A431-A6). A431wt and A431-A6 cells were starved overnight, incubated ± 10 ng EGF/ml for 3 min and cell lysates were analyzed for tyrosine (pY-EGFR) and pT654-EGFR phosphorylation (Fig. 1A-B). Alike earlier studies [34], EGF-stimulated A431-A6 cells were characterized by reduced pY-EGFR levels (Fig. 1A), while pT654-EGFR phosphorylation was strongly increased compared to EGF-treated A431wt controls (Fig. 1B).

We next determined EGFR tyrosine and T654 phosphorylation in A431-A6 cells upon PKCα depletion, using overnight incubation with phorbol esters (TPA), a common approach to attenuate PKC isozyme expression [33, 34], and shRNA-mediated PKCα knockdown (Fig. 1C-D). Indeed, PKCα depletion restored EGF-inducible EGFR tyrosine phosphorylation and Erk1/2 activity in A431-A6 cells, while pT654-EGFR phosphorylation in A431-A6 cells lacking PKCα was strongly reduced (Fig. 1C-D).

Annexin A6-induced and PKCα-mediated T654-EGFR phosphorylation inhibits EGFR activity *in vivo*

A431 xenografts are an established model to study oncogenic EGFR activity *in vivo* [37, 38] and we examined, if AnxA6-mediated inhibition of A431 tumor growth was associated with increased pT654-EGFR phosphorylation *in vivo*. Therefore, A431wt and A431-A6 cells ± stable PKCα knockdown [34] were injected subcutaneously into the flanks of nude mice (n = 5 per group) and 12 days after injection, the mean tumor mass was determined (Fig. 2A). Alike previous data [39], A431-A6 cells gave rise to significantly less tumor mass compared to A431wt (0.074 ± 0.01 g vs 0.027 ± 0.009 g). In support of PKCα knockdown restoring A431-A6 cell growth [34], PKCα depletion increased A431-A6 tumor mass approximately 4.8 -fold (0.13 ± 0.015 g). Interestingly, in AnxA6-deficient A431wt xenografts, tumor mass also increased upon PKCα depletion (3.6 –fold; 0.27 ± 0.048 g), indicating additional and AnxA6-independent growth-regulatory roles for PKCα contributing to A431wt xenograft growth.

To address if A431-A6 cells would display reduced EGFR signaling activity *in vivo*, possibly in a PKCα-dependent manner, A431wt and A431-A6 xenografts ± stable PKCα knockdown were analysed for EGFR T654 and tyrosine phosphorylation by western blotting (Fig. 2B).

Strikingly, pT654-EGFR levels in A431-A6 tumors were significantly elevated (9.9 ± 2.7 –fold) compared to A431wt xenografts (Fig. 2B compare lane 1-5 and 11-15; for quantification see Fig. 2C). In contrast, PKCα depletion in A431-A6 xenografts was associated with a significant loss of pT654-EGFR phosphorylation and comparable to pT654-EGFR levels in A431wt tumors (compare lanes 1-10 and 16-20). In support of PKCα facilitating EGFR inactivation in A431-A6 cells *in vivo*, EGFR tyrosine phosphorylation was completely attenuated in A431-A6 tumors (Fig. 2B, lanes 11-15). Moreover, PKCα depletion in A431-A6 tumors strongly increased pY-EGFR levels (4 –fold; lane 16-20), which was comparable to the magnitude of EGFR tyrosine phosphorylation displayed by A431wt tumors (lane 1-5, for quantification see Fig. 2C). Hence, upregulation of the AnxA6 scaffold in A431 cells creates a cellular environment that enables PKCα to downregulate EGFR activity *in vivo*.

Annexin A6 alters the activity of EGFR effector pathways in A431 xenografts

In line with our previous studies [30-32, 34], and the reduced EGFR tyrosine phosphorylation in A431-A6 tumors (see above), Erk1/2 phosphorylation was also reduced by 59 ± 0.5 % in A431-A6 xenografts compared to A431wt (Fig. 2B, compare lane 1-5 and 11-15, for quantification see Fig. 2C). In contrast, PKCα depletion in A431-A6 tumors increased Erk1/2 phosphorylation more than 4 -fold compared to A431-A6 scramble controls (compare lane 11-15 and 16-20). In A431-A6 tumors ± PKCα knockdown, these changes in Erk1/2 phosphorylation correlated strongly with those observed for pY-EGFR levels, indicating that elevated AnxA6 levels in A431 cells reduced MAPK activity through PKCα-mediated EGFR inactivation. Interestingly, A431wt control xenografts showed greater Erk1/2 activity compared to tumors from PKCα-depleted A431wt (Fig. 2B, compare lane 1-5 and 6-10). As A431wt xenograft mass is increased upon PKCα depletion (Fig. 2A), this further supports additional growth-regulatory roles for PKCα [24, 40-43] that are prominent only when the AnxA6 scaffold is not expressed.

The phosphoinositide 3-kinase/Akt pathway also contributes to tumor growth and progression and is a well-established EGFR effector [2-4, 10-12]. Yet, despite the inhibitory role of AnxA6 on EGFR activity, the levels of Akt serine 473 phosphorylation (P-Akt; pS473-Akt) did not correlate with EGFR tyrosine phosphorylation patterns in both A431wt and A431-A6 tumors. In fact, pS473-Akt levels were elevated in A431-A6 tumors, and PKCα depletion strongly increased Akt phosphorylation in A431wt, but not A431-A6 xenografts, indicating a

novel, yet undefined role for AnxA6, possibly involving PKCα, in Akt signaling in EGFR overexpressing cells.

Annexin A6 overexpression increases the efficacy of EGFR-TKIs to reduce A431 cell growth

Based on the findings described above, we hypothesized that AnxA6 expression could improve the efficacy of TKIs to reduce A431 cell growth. Therefore, A431wt and A431-A6 cells were grown in the presence or absence of EGFR-TKIs and colorimetric cell viability assays were performed (Fig. 3A). To abrogate EGFR signaling, EGFR-TKIs are commonly used at ≤ 10 µM in cell culture studies [44, 45], which is within or somewhat higher than the range of serum concentration observed in patients (0.4 – 1.4 µM gefitinib; 0.5 – 2.9 µM erlotinib) [46, 47]. Treatment with 5 µM gefitinib reduced cell viability to 51.8 ± 0.6 % in A431wt cells, while A431-A6 cells displayed significantly greater growth inhibition (37.7 ± 1.9 %). Similarly, 5 µM erlotinib more effectively inhibited viability of A431-A6 cells (49.6 ± 5.1 %) compared to A431wt controls (59.0 ± 5 %). Likewise, treatment with 10 µM tyrophostin (AG1478) reduced cell viability to 81.2 ± 2.5 % in A431wt cells, while A431-A6 cells displayed significantly greater growth inhibition (51.8 ± 4.2 %).

In support of our hypothesis, PKCα depletion in A431-A6 cells compromised the growth inhibitory effect of gefitinib in A431-A6, but not A431wt cells (Fig. 3B), pointing at potentially other growth-regulatory roles for PKCα [40-43] in the absence of the AnxA6 scaffold.

EGFR-TKIs more effectively lower A431 colony formation upon AnxA6 upregulation

Next, A431wt and A431-A6 cells were incubated ± 1 - 25 µM erlotinib or gefitinib for five days to allow colony formation and then colonies of twenty or more cells were determined (Fig. 3C). Alike our previous findings [34], clonogenic growth of untreated A431-A6 was strongly reduced (≥ 50 %) compared to A431wt controls. While 10 - 25 µM erlotinib almost completely inhibited colony growth in both cell lines, 1 µM erlotinib more effectively reduced colony formation in A431-A6 cells compared to A431wt cells (48 ± 2 vs 120 ± 4 colonies). Likewise, incubation with 1 µM gefitinib led to less colony formation in A431-A6 cells compared to A431wt control cells (90 ± 9 vs 143 ± 4 colonies; Fig. 3D). Taken together, the growth inhibitory effect of AnxA6 seems to cooperate with EGFR-TKI activity to effectively lower A431 colony formation.

AnxA6 reduces A431 cell migration in a PKCα-dependent manner

We next compared the migratory behaviour of A431wt and A431-A6 cells ± stable PKCα knockdown (Fig. 4A-B) and ± EGF (Fig 4. C-D) in wound healing assays.

In line with previous studies [35], A431wt showed much greater wound closure compared to A431-A6 cells after 12 h (65.6 ± 2.2 % vs. 23.8 ± 1.7) and 24 h (94.6 ± 3.4 % vs. 30.4 ±1.7 %) (Fig. 4A, for quantification see B). Alike different growth-regulatory roles for PKCα in A431wt and A431-A6 described above [34] (Fig. 2, 3B), PKCα depletion restored wound closure only in A431-A6 cells at 12 h (41.7 ± 3.4 %) and 24 h (51.6 ± 8.1 %), but not in A431wt, indicating that PKCα-mediated EGFR inactivation contributes to reduce cell motility in A431-A6 cells, but not A431wt cells (Fig. 4A, for quantification see B). We then also compared EGF-inducible cell migration in A431wt and A431-A6 cells (Fig. 4C-D). Indeed, A431wt cells displayed a more than 2 -fold greater EGF-inducible wound closure compared to A431-A6 cells after 6 h (28.1 ± 1.6 % vs. 13.4 ± 2.8 %) (Fig. 4C, for quantification see D). EGF-inducible A431-A6 cell migration was still reduced at later time points compared to A431wt controls by 31.1 % (12 h: 58.2 ± 2.2 % vs. 40.2 ± 4.7 %) and 14.6 % (24 h: 85.8 ± 2.5 vs. 74.1 ± 5.7), respectively. These findings further warrant AnxA6 not only inhibiting EGFR-inducible cell growth, but also EGFR-inducible cell migration.

Annexin A6 overexpression increases the efficacy of EGFR-TKIs to reduce A431 cell migration

Then wound healing assays with A431wt and A431-A6 ± 2 - 5 µM erlotinib and gefitinib were performed (Fig. 5A, for quantification see B). In A431wt cells, 2 - 5 µM erlotinib significantly reduced wound closure approximately 2 -fold compared to controls (71.9 ± 3.5 % vs. 30.7 ± 7.5 % and 35.5 ± 5.8 %, respectively). Yet, in A431-A6 cells, a stronger reduction in wound closure with 2 - 5 µM erlotinib was observed (46.2 ± 4 % vs. 17.4 ± 9.4 % and 26.8 ± 0.6 %). Similarly, 2 - 5 µM gefitinib reduced wound closure more than 2 -fold in A431wt (71.9 ± 3.5 % vs. 30.8 ± 4.5 % and 28 ± 6.1 %, respectively). Yet again, gefitinib more effectively inhibited A431-A6 cell migration (46.2 ± 4 % to 11.8 ± 5 % and 15.8 ± 8.5 %, respectively) (Fig. 5A-B). In line with a minor involvement of PKCα in A431wt and A431-A6 cell migration (see quantification in Fig. 4B), inhibition of wound closure in the presence of 5 µM erlotinib and gefitinib was comparable in both cell lines ± PKCα (not shown). Taken together, EGFR-TKIs more effectively inhibited A431 cell migration upon AnxA6 upregulation, yet the role of PKCα in this process is minor.

AnxA6 promotes TKI-mediated inhibition of A431 cell invasion

TKIs can reduce EGFR-related tumor cell invasion [48, 49] and we next examined cell motility, using Incucyte, of A431wt and A431-A6 cells ± TKIs through a wound coated with matrigel (Fig. 6). In control experiments, migration on uncoated 96-well plates was determined after 24 h and similar to the results obtained from wound healing assays (Fig. 5A-B), erlotinib and gefitinib inhibited A431wt cell migration by approximately 30 - 35 % (Fig. 6A-B). Migration of A431-A6 cells was strongly reduced (~ 2-fold) compared to A431wt cells, and both gefitinib and erlotinib decreased migration in AnxA6 expressing cells ~ 2 - 3-fold more effectively compared to controls.

Incubation with gefitinib and erlotinib strongly reduced the number of invading A431wt cells in matrigel coated wells (Fig. 6C-D). Strikingly, A431-A6 cell invasion was reduced by 15 - 20 % compared to A431wt cells and decreased 1.5 - 2.9 -fold further in the presence of erlotinib and gefitinib compared to drug-treated A431wt cells. Hence, the tumor suppressive activity of AnxA6 appears to substantially improve the anti- invasive properties of TKIs in EGFR overexpressing A431 cells.

AnxA6 increases TKI-mediated inhibition of A431 cell sprouting in 3D spheroids

Finally, we compared invasive properties of A431wt and A431-A6 cells ± TKIs in 3D-spheroids, which mimic some features of solid tumors and have been proven valuable *in vitro* models for screening anticancer therapeutics [50] (Fig. 7A, for quantification see B). Therefore, A431wt and A431-A6 spheroids were incubated ± 0.1 - 10 µM gefitinib and erlotinib for 7 or 22 days (Fig. 7C). At concentrations higher than 1 µM, there was a trend that both TKIs inhibited A431-A6 spheroid growth slightly more effective compared to the A431wt cells (Fig. 7B). Strikingly, A431-A6 cells displayed a strongly reduced ability to invade the surrounding matrix (sprouting). Gefitinib only displayed anti-invasive efficacy in A431-A6, but not A431wt cells (Fig. 7C). On the other hand, erlotinib strongly reduced sprouting in A431wt cells, although invasive properties in erlotinib-treated A431-A6 were still lowest (Fig. 7C). Thus, together with the matrigel assays described above (Fig. 6C-D), these findings point at the reduced invasive features of AnxA6 expressing A431 cells, which contribute to improve the anti-migratory and anti-invasive properties of TKIs.

Discussion

Here we demonstrate that restoration of AnxA6 expression in A431 cells, which lack endogenous AnxA6, reduces EGFR activity in a PKCα-dependent manner *in vivo*. Furthermore, the ability of the scaffolding function of AnxA6 to impede growth, migration and invasion of EGFR overexpressing squamous epithelial A431 carcinoma cells improves growth-inhibitory, but also anti-migratory and anti-invasive properties of pharmacological EGFR inhibitors (gefitinib, erlotinib).

The requirement of PKCα for AnxA6-dependent EGFR inactivation *in vivo* and the differential TKI response of PKCα-depleted A431wt and A431-A6 cells highlights the complexity of PKCα-related biological activities [9, 24, 51]. In fact, the manifold interaction partners and functions of PKCα in growth, survival and motility probably account for varied tumor-promoting or tumor-suppressing activities, depending on the cell type and local environment [9, 24, 51]. As evident from the studies described here and previously [23, 24, 34], restoration of AnxA6 scaffold expression in the A431 cell line serves as a switch to facilitate the involvement of PKCα in EGFR signal termination *in vivo*. We and others have recently summarized the changes in expression levels of annexins, including AnxA6, in cancer and other disease settings [23-28, 34, 52]. Hence, AnxA6 up-or downregulation is likely to influence the subcellular location of PKCα, with consequences not only for the activity, but also the localization and trafficking of PKCα interaction partners, including EGFR. Indeed, AnxA6-induced and PKCα-mediated T654-EGFR phosphorylation strongly reduced EGFR internalization and trafficking to lysosomes for degradation [34, 53, 54]. Thus, the presence or absence of AnxA6/PKCα protein complexes induce changes in the intracellular fate of EGFR that could ultimately also affect susceptibility for drugs targeting the EGFR-TK domain.

A431 cells are a well-recognized model for the testing of pharmacological drugs targeting EGFR [37, 38], originate from an epidermoid cancer and display highly elevated EGFR expression levels. Hence, researchers have extensively used this cell line to simulate TKIs targeting EGFR in other squamous cell carcinomas such as NSCLC and HNSCC. Hence, one can speculate that increased TKI efficacy to inhibit cell growth, migration and invasion in AnxA6 expressing A431 cells could be relevant for other epidermoid cancers. In fact, these observations may represent a common theme, as several other scaffolds in squamous cell carcinomas from head and neck or lung cancers also seem to augment or downregulate signal

output due to their impact on EGFR localization and trafficking, with consequences for EGFR-drug interactions. For instance, increased dissociation of gefitinib from the EGFR due to their accumulation in low-pH endosomes could be responsible for reduced drug effectiveness in head and neck squamous carcinoma cells overexpressing cortactin [14]. On the other hand, reduced interaction of caveolin-1 with EGFR may trigger EGFR redistribution at the cell surface and/or alter EGFR internalization/recycling kinetics, thereby contributing to increased EGFR-TKI sensitivity of a lung adenocarcinoma cell line [18]. Other scaffolds may modulate the number of accessible and drug-sensitive EGFR-containing complexes at the cell surface. For example, loss of the Aki1 scaffold protein, which stabilizes and potentiates mutant EGFR signaling, improved the growth inhibition of EGFR mutant lung cancer cells treated with new generation EGFR-TKIs [17]. Similarly, scaffold proteins which assemble signal complexes downstream of EGFR at the cell surface and possibly endosomal compartments, including kinase suppressor of Ras and IQ Motif Containing GTPase Activating Protein 1, alter the performance of drugs targeting the Ras/MAPK pathway [15, 20, 55].

Based on these observations, one could envisage that expression patterns of scaffold proteins could potentially serve as markers to develop molecular profiles from individual tumors for better treatment strategies and prediction of treatment outcome. Indeed, upregulated cortactin levels not only confer resistance to EGFR-TKIs in cell-based studies [14], but also have potential to predict local recurrence, disease-free survival and overall survival in head and neck cancers independent of EGFR expression status [56]. Also, caveolin-1 levels have been associated with drug resistance in a number of different cancers, including acquired drug resistance to EGFR-TKIs in lung cancers carrying EGFR mutations [18]. Likewise, significant Alk1 levels were detected in all lung tumors from a small cohort of patients with acquired resistance to EGFR-TKIs [17]. Along these lines, several annexins may have the capacity to become markers for treatment outcome of EGFR-related cancers. AnxA1 stimulates inward vesiculation in multivesicular bodies, a final step in lysosomal EGFR degradation, and controls the recruitment of the protein-tyrosine phosphatase 1B to EGFR [5, 21-23]. Its downregulation correlates with poor prognosis in head and neck cancers, where prevalence of EGFR overexpression is common [57]. Interestingly, AnxA1 may also serve as a biomarker for the trastuzumab-resistance of ErbB2 (Her2) -positive breast cancers [58]. AnxA2 likely controls actin-membrane dynamics to enable lateral EGFR movements at the cell

surface and/or EGFR internalization and sorting in early endosomes [22, 23, 26]. Elevated AnxA2 levels correlate with poor survival and may moderate resistance to EGFR-directed therapy in triple negative breast cancer [59, 60]. In addition, AnxA2 together with EGFR, is reciprocally regulated to ErbB2 in Herceptin-resistant breast cancers [61] and seems to contribute to the acquired resistance of non-small cell lung cancers to EGFR-TKIs [62].

AnxA6 exhibits tumor-suppressor as well as tumor-promoting activities, depending on the type and degree of malignancy [23, 27, 28, 52], making attempts to develop AnxA6 as a biomarker difficult. We and others identified a correlation between loss of AnxA6 and elevated EGFR activity in various settings [25, 30, 31, 34, 37], yet these observations might only be relevant for subtypes of certain cancers, as indicated by the variability in TKI response observed after AnxA6 up- and downregulation in several cancer models [25, 34, 63]. For example, recent studies in estrogen-receptor negative breast cancer cell lines identified AnxA6 depletion to sensitize BT-549, but not MDA-MB-231 cells, to EGFR-TKIs in cell viability assays [25]. On the other hand, studies presented here show AnxA6 upregulation in EGFR overexpressing human squamous epithelial cells to increase efficacy of EGFR-TKIs to reduce growth, migration and invasion. Probably the cell-specific expression patterns of AnxA6 interaction partners, such as EGFR, PKCα, but also H-Ras and p120GAP are underlying causes, creating different scenarios and scaffolding functions for AnxA6 in the various cell models analyzed [23, 24, 26-28, 32]. While our previous analysis of a small breast cancer patient cohort did not identify a correlation between AnxA6 levels and EGFR activity in luminal, ErbB2-positive or basal-like tumors [34], others identified low AnxA6 levels to be associated with higher recurrence-free survival in basal-like breast cancers [25]. Hence, AnxA6 downregulation may indeed serve as a biomarker in some cancer subtypes.

Most interestingly, studies presented here identified that elevated AnxA6 levels strongly reduced A431 cell motility in 3D-migration/invasion assays, which potentiated the anti-invasive properties of EGFR-TKIs. The role of PKCα appeared minor in this process, indicating that in addition to AnxA6/PKCα -mediated EGFR inactivation, other AnxA6 functions may cooperate to modulate migratory and invasive A431 cell behavior. Indeed, the AnxA6 interactome includes a plethora of proteins that contribute to determine the tumor microenvironment, such as the extracellular matrix and exosomes, but also cell motility via membrane lipids, Ca^{2+} signaling, the cytoskeleton, and cell signaling [63]. In addition, we recently identified that accumulation of cholesterol in late endosomes, which can be

induced by AnxA6 overexpression [31], led to reduced cell migration and invasion of A431 cells and several other cell lines [35, 64]. In these and previous other studies from our group, AnxA6-induced late endosomal cholesterol accumulation strongly reduced the recycling of integrins to the cell surface [35, 64], secretion of the extracellular matrix protein fibronectin [65], and the transport of caveolin to the cell surface [29], all of which critical for cell motility. The blockage of late endosomal cholesterol export in AnxA6 expressing cells led to a significant reduction of caveolae and cell surface cholesterol levels, with concomitant lipid re-distributions at the plasma membrane, even in live cells [31, 66]. These findings coincide with the distribution of EGFR at the cell surface, which is often being found in highly specialized and cholesterol-rich microdomains ('lipid rafts', caveolae). Although the role of cholesterol-rich domains for EGFR signaling is not fully understood [23, 67], several studies identified statin- or methylcyclodexrin-induced cholesterol depletion, which disrupts cholesterol-rich domains at the cell surface, to increase sensitivity to EGFR-TKIs [68, 69]. Interestingly, prolonged treatment of triple-negative breast cancer cells with lapatinib, a new generation EGFR and ErbB2 inhibitor, caused cholesterol accumulation in late endosomes that was accompanied by AnxA6 upregulation [70], further highlighting the close relationship between EGFR localization and activity, cellular cholesterol transport and AnxA6 expression. Hence, it is tempting to speculate that AnxA6-induced changes in cholesterol distribution at the cell surface and endosomal compartments could contribute to alter the distribution of EGFR in specialized microdomains, with consequences for the accessibility and sensitivity to EGFR-TKIs.

In conclusion, the up- or downregulation of the scaffold protein AnxA6 is associated with changes in EGFR activity, leading to alterations in the growth-inhibitory, but also anti-migratory and anti-invasive properties of TKIs. Further research will be required to determine if increased TKI efficacy in AnxA6 expressing A431 cells leads to improved anti-metastatic properties of TKIs *in vivo*. This study, using A431 squamous epithelial cells as a model, adds to several recent observations on the molecular consequences associated with AnxA6 up- or downregulation that may add to a better understanding of disease severity, progression and treatment outcome for other epidermoid cancer subtypes [25, 57, 70-72]. Moreover, pharmacological manipulation of AnxA6 levels, such as the recently described glucocorticoid-steroid dosing [73], or directly targeting AnxA6 function [74], may provide opportunities to improve anticancer treatment strategies.

Materials and Methods

Reagents and antibodies

DMEM, trypsin, L-glutamine, penicillin, streptomycin were from Invitrogen. Geneticin (G418) and human recombinant EGF were from Merck. 2-mercaptoethanol, 12-O-tetradecanoyl-phorbol-13-acetate (TPA), puromycin, dimethylsulfoxide (DMSO) were from Sigma. EGFR-TKIs (gefitinib, erlotinib, AG1478) were from Cayman Chemicals. Mono- and polyclonal antibodies against EGFR, rabbit anti-pT654-EGFR were from Santa Cruz. Mouse monoclonal antibodies against PKCα were from BD Transduction Laboratories. Antibodies against phosphotyrosine (mouse), activated extracellular signal-regulated kinase 1/2 (P-Erk1/2; mouse) and protein kinase B (P-Akt, Ser473; rabbit), Total Erk1/2 (rabbit) and Akt (rabbit), and β-actin (rabbit) were from Cell Signaling. The rabbit anti-AnxA6 antibody was prepared in our laboratory [75, 76]. Horseradish Peroxidase (HRP) -labeled antibodies and SDS-PAGE molecular weight markers were from Cell Signaling.

Cell culture

A431wt and A431-A6 were grown in DMEM together with 10% fetal calf serum (FCS), L-glutamine (2 mM), penicillin (100 U/ml) and streptomycin (100 μg/ml) at 37 °C, 5 % CO_2. A431wt and A431-A6 cell lines stably expressing scrambled or PKCα-targeting shRNA were grown in the presence of 1.5 μg/ml puromycin. The generation of A431 cells stably expressing AnxA6 and the A431wt and A431-A6 cell lines stably expressing scrambled or PKCα-targeting shRNA has been described [30, 34].

Suppression of PKCα expression by RNA interference

For stable PKCα knockdown, 1 - 2 x 10^6 cells were transfected with 1.5 μg SureSilencing shRNA plasmid (SABiosciences) targeting human PKCα at Pos. 1606-1626 (5'-cctccatttgatggtgaagat-3') together with Lipofectamine 2000 (Invitrogen), according to the manufacturer's instructions [34]. After 48 h, cells were selected with 1.5 μg/ml puromycin. After 2 weeks, puromycin-resistant and PKCα-depleted colonies were identified. Stable A431wt and A431-A6 expressing scrambled shRNA (5'-ggaatctcattcgatgcatac-3') served as negative controls. PKCα depletion was confirmed in lysates of isolated colonies by western blotting (~ 70 – 90 %; see also Fig. 1D and 2A).

Growth assays

Cell proliferation was determined using the colorimetric CellTiter 96® AQueous Cell Proliferation Assay Kit (MTS, 3-(4,5-dimethylthiazol-2-yl)-5-(3-carboxymethoxyphenyl)-2-(4-sulfophenyl)-2H-tetrazolium; PMS, phenazine methosulfate) according to the manufacturer's (Promega) instructions. 5 x 10^3 cells were seeded in 96-well plates and grown ± TKIs (0 – 10 µM) for 72 h. Then cells were incubated with MTS/PMS solution (20:1) for 4 h, and spectrophotometric absorbance of samples was measured at 490 nm (Microplate Reader, Model 689, Biorad) [34]. All experiments were performed in triplicate in at least 3 separate experiments.

Colony forming assays were performed as described [34]. 8 x 10^3 cells were grown in 6-well plates and treated ± EGFR-TKIs (0 - 25 µM) for 5 days. Cells were washed twice with PBS and fixed and stained with Diff Quick Stain (Lab Aids, Australia) according to manufacturer instructions. Cells were viewed with the PALM Duoflex Combi System and images were collected using a 5 x objective (PALM Robo Software). Colonies (> 20 cells) were quantified using ImageJ Analysis Software (v1.47).

A431 xenograft analysis

Xenografts from A431wt and A431-A6 ± PKCα knockdown cells were prepared and monitored as described [77]. In brief, 3 - 6 x 10^6 cells were injected subcutaneously into immunosuppressed nude mice. Five mice per cell line were analysed. The mice were weighed at baseline (t = 0) and daily for 2 weeks. Mice were then sacrificed, tumors removed and weighed as described [77]. Tumor sections were sonicated on ice in lysis buffer (20 mM Tris-HCl, pH 7.5, 2 mM EDTA, 100 mM NaCl, 5 mM $MgCl_2$, 1 % (v/v) Triton X-100, 5 mM NaF, 10 % (v/v) glycerol, 0.5 % (v/v) 2-mercaptoethanol, 0.1 mM Na_3VO_4, 1 mM phenylmethylsulfonyl fluoride, 5 µg/mL leupeptin and 2 µg/mL aprotinin) for 5 - 10 min. After centrifugation at 10,000 g for 5 min at 4 °C, the protein concentration of the cleared cell lysate was determined. Tissue samples were then analysed via western blotting for phosphorylated and total EGFR, Erk1/2 and Akt. All animal work was carried out according to the animal protocol approved by the Garvan/St Vincent's Hospital Animal Ethics Committee (Animal ethics number 11/46) and conducted in accordance with national (NHMRC) guidelines for the ethical treatment of animals.

Western blot analysis

Cells were harvested in lysis buffer (20 mM Tris-HCl, pH 7.5, 2 mM EDTA, 100 mM NaCl, 5 mM $MgCl_2$, 1 % (v/v) Triton X-100, 5 mM NaF, 10% (v/v) glycerol, 0.5 % (v/v) 2-mercaptoethanol, 0.1 mM Na_3VO_4 and protease inhibitors). After centrifugation at 10,000 g for 5 min at 4 °C the protein concentration of the cleared cell lysate was determined. Cell and tissue lysates (see above) were separated by 8 - 12.5 % SDS-PAGE and transferred to Immobilon-P (Millipore). Proteins were detected using their specific primary antibodies, followed by HRP-conjugated secondary antibodies and enhanced chemiluminescence detection (ECL, Perkin-Elmer).

Wound healing assays

6-well plates were marked with horizontal lines at the base of the plate. 5×10^5 cells were seeded in triplicate and grown until ~90 % confluence. Cells were incubated ± pharmacological EGFR inhibitors (0 – 5 µM) and scratches were made using a 200 µL pipette tip across the center of each well, such that the scratches were perpendicular to the marked horizontal lines [35, 64]. Images were acquired immediately after scratching (t = 0) and post-scratch every 4 - 6 h for 2 days, until cells completely covered the scratched area. Cells were washed at each time point to remove possible cell debris and non-adherent cells. Scratches were studied at 10 x magnification using a Nikon Eclipse TS100 inverted microscope, and images were collected with Leica Microsystems Digital Imaging. Image analysis was performed with ImageJ software. The area of the scratch was calculated for the various time points as percent reduction in area over time (RWD %). Three independent experiments in triplicate per cell line were performed.

Matrigel invasion assays

Cell invasion was analyzed using MatriGel Matrix (BD Falcon) as described [78]. A431wt and A431-A6 cells (2×10^3 cells/well) were seeded in 96-well plates (IncuCyte) and after 24 h, each well was scratched using the WoundMaker (IncuCyte). Cell debris was removed and 45 µL of MatriGel Matrix was added to each well and allowed to solidify for 30–60 min. Once the Matrigel Matrix was set, cells were treated ± pharmacological EGFR inhibitors (0 - 1 µM). As control, cell migration (± EGFR-TKIs) in the absence of MatriGel Matrix was also determined.

The plates were imaged over 72 h (IncuCyte), and the relative wound density (RWD %) was analyzed with IncuCyte Zoom software.

Spheroid growth

Spheroidal growth assays were performed as described [79]. In brief, 2 x 10^3 cells/well were plated on an agarose-coated 96-well plate. Cells were centrifuged at 200 g for 3 min and incubated for 48 h to allow spheroid formation. Spheroids were incubated with 0 - 10 µm gefitinib or erlotinib for additional 7 or 22 days. Growth and sprouting (relative to area of spheroid on day 1) were monitored with an inverted microscope (10 x magnification) every 5 - 7 days and quantified for each spheroid with ImageJ as described [79].

Statistics

Statistical analysis was carried out using Microsoft Excel (Redmond, WA, USA) and Graph Pad Prism 6 (Graphpad, La Jolla, CA, USA). Data represent means of at least 3 independent biological experiments with triplicate samples in each experiment, and unless stated otherwise, error bars show the standard error of the mean (SEM). T-test values represent the results from unpaired, two tailed Student's *t*-tests. * = $p < 0.05$, ** = $p < 0.01$, *** = $P < 0.001$, **** = $P < 0.0001$.

Author contribution

M.H., Y.A.E., M.K., S.S.B, J.J., E. M.-S. and P.B.-M. performed the experiments, prepared reagents and analysed the data. J.R.W.C., A.S. and P.T. performed experiments and contributed reagents and other essential material. F.T., C.E., C.R. and T.G. planned the experiments and wrote the manuscript.

Acknowledgements

T.G. is supported by the University of Sydney (U7007, U7042, U7113, RY253), Sydney, Australia. C.E. is supported by grants from the Ministerio de Economía y Competitividad (BFU2015-66785-P and CSD2009-00016) and Fundació Marató TV3 (PI042182), Spain. C.R. is supported by the Serra Húnter programme (Generalitat de Catalunya). P. T. is supported by a Len Ainsworth Fellowship in Pancreatic Cancer Research, is an NHMRC Senior Research Fellow and is supported by NHMRC projects grant, Suttons Motors and Sydney Catalyst. We are grateful to Fiona Simpson (Diamantina Institute, University of Queensland) for technical advice and critical reading of the manuscript and Andrea McFarland (Garvan Institute of Medical Research) for technical assistance with the animal studies.

References

1. Burgess AW, Cho HS, Eigenbrot C, Ferguson KM, Garrett TP, Leahy DJ, Lemmon MA, Sliwkowski MX, Ward CW & Yokoyama S (2003) An open-and-shut case? Recent insights into the activation of EGF/ErbB receptors. *Mol Cell* 12, 541-552.
2. Bergeron JJ, Di Guglielmo GM, Dahan S, Dominguez M & Posner BI (2016) Spatial and temporal regulation of receptor tyrosine kinase activation and intracellular signal transduction. *Annu Rev Biochem* 85, 573-597.
3. Bakker J, Spits M, Neefjes J & Berlin I (2017) The EGFR odyssey – from activation to destruction in space and time. *J Cell Sci* 130, 4087-4096.
4. Tomas A, Futter CE & Eden ER (2014) EGF receptor trafficking: consequences for signaling and cancer. *Trends Cell Biol* 24, 26-34.
5. Eden ER, White IJ, Tsapara A & Futter CE (2010) Membrane contacts between endosomes and ER provide sites for PTP1B-epidermal growth factor interaction. *Nat Cell Biol* 12, 267-272.
6. Hunter T, Ling N & Cooper JA (1984) Protein kinase C phosphorylation of the EGF receptor at a threonine residue close to the cytoplasmic face of the plasma membrane. *Nature* 311, 480-483.
7. Livneh E, Dull TJ, Berent E, Prywes R, Ullrich A & Schlessinger J (1988) Release of a phorbol ester-induced mitogenic block by mutation at Thr-654 of the EGFR. *Mol Cell Biol* 8, 2302-2308.
8. Fabbro D, Küng W, Roos W, Regazzi R & Eppenberger U (1986) Epidermal growth factor binding and protein kinase C activities in human breast cancer cell lines: possible quantitative relationship. *Cancer Res* 46, 2720-2725.
9. Mackay HJ & Twelves CJ (2007) Targeting the protein kinase C family: are we there yet? *Nat Rev Cancer* 7, 554-562.
10. Wheeler DL, Dunn EF & Harari PM (2010) Understanding resistance to EGFR inhibitors on future treatment strategies. *Nat Rev Clin Oncol* 7, 493-507.
11. Pines G, Köstler WJ & Yarden Y (2010) Oncogenic mutant forms of EGFR: lessons in signal transduction and targets for cancer therapy. *FEBS Lett* 584, 2699-2706.
12. Han W & Lo HW (2012) Landscape of EGFR signaling network in human cancers: biology and therapeutic response in relation to receptor subcellular locations. *Cancer Lett* 318, 124-134.
13. Wang S & Li J (2019) Second-generation EGFR and ErbB tyrosine kinase inhibitors as first-line treatments for non-small cell lung cancer. *Onco Targets Ther* 12, 6535-6548.
14. Tagliamento M, Genova C, Rijavec E, Rossi G, Biello F, Dal Bello MG, Alama A, Coco S, Boccardo S & Grossi F (2018) Afatinib and erlotinib in the treatment of squamous-cell lung cancer. *Expert Opin Pharmacother* 19, 2055-2062.
15. Tan DSW, Chong FT, Leong HS, Toh SY, Lau DP, Kwang XL, Zhang X, Sundaram GM, Tan GS, Chang MM, Chua BT, Lim WT, Tan EH, Ang MK, Lim TKH, Sampath P, Chowbay B, Skanderup AJ, DasGupta R & Iyer NG (2017) Long noncoding RNA EGFR-AS1 mediates epidermal growth factor receptor addiction and modulates treatment response in squamous cell carcinoma. *Nat Med* 23, 1167-1175.
16. Cohen EE, Davis DW, Karrison TG, Seiwert TY, Wong SJ, Nattam S, Kozloff MF, Clark JI, Yan DH, Liu W, Pierce C, Dancey JE, Stenson K, Blair E, Dekker A & Vokes EE (2009) Erlotinib and bevacizumab in patients with recurrent or metastatic squamous-cell carcinoma of the head and neck: a phase I/II study. *Lancet Oncol* 10, 247–257.

13. Arteaga CL & Engelman JA (2014) ERBB receptors: from oncogene discovery to basic science to mechanism-based cancer therapeutics. *Cancer Cell* 25, 282-303.
14. Timpson P, Wilson AS, Lehrbach GM, Sutherland RL, Musgrove EA & Daly RJ (2007) Aberrant expression of cortactin in head and neck squamous cell carcinoma cells is associated with enhanced cell proliferation and resistance to the EGFR inhibitor gefitinb. *Cancer Res* 67, 9304-9314.
15. Neilsen BK, Frodyma DE, Lewis RE & Fisher KW (2017) KSR as a therapeutic target for Ras-dependent cancers. *Expert Opin Ther Targets* 21, 499-509.
16. Kolch W (2005) Coordinating ERK/MAPK signaling through scaffolds and inhibitors. *Nat Rev Mol Cell Biol* 6, 827-837.
17. Yamada T, Takeuchi S, Fujita N, Nakamura A, Wang W, Li Q, Oda M, Mitsudomi T, Yatabe Y, Sekido Y, Yoshida J, Higashiyama M, Noguchi M, Uehara H, Nishioka Y, Sone S & Yano S (2013) Akt kinase-interacting protein 1, a novel therapeutic target for lung cancer with EGFR-activating and gatekeeper mutations. *Oncogene* 32, 4427-4435.
18. Cui Y, Zhu T, Song X, Liu J, Liu S & Zhao R (2018) Downregulation of caveolin-1 increased EGFR-TKIs sensitivity in lung adenocarcinoma cell line with EGFR mutation. *Biochem Biophys Res Commun* 495, 733-739.
19. Agelaki S, Spiliotaki M, Markomanolaki H, Kallergi G, Mavroudis D, Georgoulias V & Stournaras C (2009) Caveolin-1 regulates EGFR signaling in MCF-7 breast cancer cells and enhances gefitinib-induced tumor cell inhibition. *Cancer Biol Ther* 8, 1470-1477.
20. McKay MM, Freeman AK & Morrison DK (2011) Complexity in KSR function revealed by Raf inhibitor and KSR structure studies. *Small GTPases* 2, 276-281.
21. Eden ER, Sanchez-Heras E, Tsapara A, Sobota A, Levine TP & Futter CE (2016) Annexin A1 tethers membrane contact sites that mediate ER to endosome cholesterol transport. *Dev Cell* 37, 473-483.
22. Futter CE & White IJ (2007) Annexins and endocytosis. *Traffic* 8, 951-958.
23. Grewal T & Enrich C (2009) Annexins--modulators of EGF receptor signaling and trafficking. *Cell Signal* 21, 847-858.
24. Hoque M, Rentero C, Cairns R, Tebar F, Enrich C & Grewal T (2014) Annexins – scaffolds modulating PKC localization and signaling. *Cell Signal* 26, 1213-1225.
25. Koumangoye RB, Nangami GN, Thompson PD, Agboto VK, Ochieng J & Sakwe AM (2013) Reduced annexin A6 expression promotes the degradation of activated epidermal growth factor receptor and sensitizes invasive breast cancer cells to EGFR-targeted tyrosine kinase inhibtors. *Mol Cancer* 12, 167.
26. Gerke V, Creutz CE & Moss SE (2005) Annexins: linking Ca2+ signaling to membrane dynamics. *Nat Rev Mol Cell Biol* 6, 449-461.
27. Enrich C, Rentero C, Vilà de Muga S, Reverter M, Mulay V, Wood P, Koese M & Grewal T (2011) Annexin A6 – linking Ca2+ signaling with cholesterol transport. *Biochim Biophys Acta – Mol Cell Res* 1813, 935-947.
28. Grewal T, Koese M, Rentero C & Enrich C (2010) Molecules in focus: Annexin A6 – regulator of the EGFR/Ras signaling pathway and cholesterol homeostasis. *Int J Biochem Cell Biol* 42, 580-584.
29. Cubells L, Vilà de Muga S, Tebar F, Wood P, Evans R, Ingelmo-Torres M, Calvo M, Gaus K, Tebar F, Pol A, Grewal T & Enrich C (2007) Annexin A6 induced alterations in cholesterol transport and caveolin export from the Golgi complex. *Traffic* 8, 1568-1589.
30. Grewal T, Evans R, Rentero C, Tebar F, Cubells L, de Diego I, Kirchhoff MF, Hughes WE, Heeren J, Rye KA, Rinninger F, Daly RJ, Pol A & Enrich C (2005) Annexin A6 stimulates the

membrane recruitment of p120GAP to modulate Ras and Raf-1 activity. *Oncogene* 24, 5809-5820.
31. Vilà de Muga S, Timpson P, Cubells L, Evans R, Hayes TE, Rentero C, Hegemann A, Reverter M, Leschner J, Pol A, Tebar F, Daly RJ, Enrich C & Grewal T (2009) Annexin A6 inhibits Ras signaling in breast cancer cells. *Oncogene* 28, 363-377.
32. Grewal T & Enrich C (2006) Molecular mechanisms involved in Ras inactivation: the annexin A6-p120GAP complex. *Bioessays* 28, 1211-1220.
33. Rentero C, Evans R, Wood P, Tebar F, Vilà de Muga S, Cubells L, de Diego I, Hayes TE, Hughes WE, Pol A, Rye KA, Enrich C & Grewal T (2006) Inhibition of H-Ras and MAPK is compensated by PKC-dependent pathways in annexin A6 expressing cells. *Cell Signal* 18, 1006-1016.
34. Koese M, Rentero C, Kota BP, Hoque M, Cairns R, Wood P, Vilà de Muga S, Reverter M, Alvarez-Guaita A, Monastyrskaya K, Hughes WE, Swarbrick A, Tebar F, Daly RJ, Enrich C & Grewal T (2013) Annexin A6 is a scaffold for PKCα to promote EGFR inactivation. *Oncogene* 32, 2858-2872.
35. García-Melero A, Reverter M, Hoque M, Meneses-Salas E, Koese M, Conway JR, Johnsen CH, Alvarez-Guaita A, Morales-Paytuvi F, Elmaghrabi YA, Pol A, Tebar F, Murray RZ, Timpson P, Enrich C, Grewal T & Rentero C (2016) Annexin A6 and late endosomal cholesterol modulate integrin recycling and cell migration. *J Biol Chem* 291, 1320-1335.
36. Smythe E, Smith PD, Jacob SM, Theobald J & Moss SE (1994) Endocytosis occurs independently of annexin VI in human A431 cells. *J Cell Biol* 124, 301-306.
37. Theobald J, Hanby A, Patel K & Moss SE (1995) Annexin VI has tumour-suppressor activity in human A431 squamous epithelial carcinoma cells. *Br J Cancer* 71, 786-788.
38. Lynch DH & Yang XD (2002) Therapeutic potential of ABX-EGF: a fully human anti-epidermal growth factor receptor monoclonal antibody for cancer treatment. *Semin Oncol* 29 (Suppl 4), 47-50.
39. Wakeling AE, Guy SP, Woodburn JR, Ashton SE, Curry BJ, Barker AJ & Gibson KH (2002) ZD1839 (Iressa): an orally active inhibitor of epidermal growth factor signaling with potential for cancer therapy. *Cancer Res* 62, 5749-5754.
40. Marais R, Light Y, Mason C, Paterson H, Olson MF & Marshall CJ (1998) Requirement of the Ras-GTP-Raf complexes for activation of Raf-1 by protein kinase C. *Science* 280, 109-112 (erratum appears in Science 280, 987).
41. Agell N, Bachs O, Rocamora N & Villalonga P (2002) Modulation of the Ras/Raf/MEK/ERK pathway by Ca(2+) and calmodulin. *Cell Signal* 14, 649-654.
42. Schönwasser DC, Marais RM, Marshall CJ & Parker PJ (1998) Activation of the mitogen-activated protein kinase/extracellular signal-regulated kinase pathway by conventional, novel and atypical protein kinase C isotypes. *Mol Cell Biol* 18, 790-798.
43. Yamaguchi K, Ogita K, Nakamura S & Nishizuka Y (1995) The protein kinase C isoforms leading to MAP-kinase activation in CHO cells. *Biochem Biophys Res Commun* 210, 639-647.
44. Kim Y, Apetri M, Luo B, Settleman JE & Anderson KS (2015) Differential effects of tyrosine kinase inhibitors in normal and oncogenic EGFR signaling and downstream effectors. *Mol Cancer Res* 13, 765-774.
45. Matar P, Rojo F, Cassia R, Moreno-Bueno G, Di Cosimo S, Tabernero J, Guzmán M, Rodriguez S, Arribas J, Palacios J & Baselga J (2004) Combined epidermal growth factor receptor targeting with the tyrosine kinase inhibitor gefitinib (ZD1839) and the

monoclonal antibody cetuximab (IMC-C225): superiority over single-agent receptor targeting. *Clin Cancer Res* 10, 6487-6501.
46. Mukohara T, Engelman JA, Hanna NH, Yeap BY, Kobayashi S, Lindeman N, Halmos B, Pearlberg J, Tsuchihashi Z, Cantley LC, Tenen DG, Johnson BE & Jänne PA (2005) Differenttial effects of gefitinib and cetuximab on non-small cell lung cancers bearing epidermal growth factor receptor mutations. *J Natl Cancer Inst* 97, 1185-1194.
47. Yeo WL, Riely GJ, Yeap BY, Lau MW, Warner JL, Bodio K, Huberman MS, Kris MG, Tenen DG, Pao W, Kobayashi S & Costa DB (2010) Erlotinib at a dose of 25 mg daily for non-small cell lung cancers with EGFR mutations. *J Thorac Oncol* 5, 1048-1053.
48. Yang Z, Bagheri-Yarmand R, Wang RA, Adam L, Papadimitrakopoulou VV, Clayman GL, El-Naggar A, Lotan R, Barnes CJ, Hong WK & Kumar R (2004) The epidermal growth factor receptor tyrosine kinase inhibitor ZD1839 (Iressa) suppresses c-Src and Pak1 pathways and invasiveness of human cancer cells. *Clin Cancer Res* 10, 658-667.
49. Li J, Kleeff J, Giese N, Büchler MW, Korc M & Friess H (2004) Gefitinib (Iressa, ZD 1839), a selective epidermal growth factor receptor tyrosine kinase inhibitor, inhibits pancreatic cancer cell growth, invasion, and colony formation. *Int J Oncol* 25, 203-210.
50. Nunes AS, Barros AS, Costa EC, Moreira AF & Correia IJ (2019) 3D tumor spheroids as in vitro models to mimic in vivo human solid tumors resistance to therapeutic drugs. *Biotechnol Bioeng* 116, 206-226.
51. Garg R, Benedetti LG, Abera MB, Wang H, Abba M & Kazanietz MG (2014) Protein kinase C and cancer: what we know and what we do not. *Oncogene* 33, 5225-5237.
52. Qi H, Liu S, Guo C, Wang J, Greenaway FT & Sun MZ (2015) Role of annexin A6 in cancer. *Oncol Lett* 10, 1947-1952.
53. Lund KA, Lazar CS, Chen WS, Walsh BJ, Welsh JB, Herbst JJ, Walton GM, Rosenfeld MG, Gill GN & Wiley HS (1990) Phosphorylation of the epidermal growth factor receptor at threonine 654 inhibits ligand-induced internalization and down-regulation. *J Biol Chem* 265, 20517-20523.
54. Bao J, Alroy I, Waterman H, Schejter ED, Brodie CH, Gruenberg J & Yarden Y (2000) Threonine phosphorylation diverts internalized epidermal growth factor receptors from a degradative pathway to the recycling endosome. *J Biol Chem* 275, 26178-26186.
55. Jameson KL, Mazur PK, Zehnder AM, Zhang J, Zarnegar B, Sage J & Khavari PA (2013) IQGAP1 scaffold-kinase interactions blockade selectively targets RAS-MAP kinase-driven tumors. *Nat Med* 19, 626-630.
56. Hofman P, Butori C, Havet K, Hofman V, Selva E, Guevara N, Santini J & Van Obberghen-Schilling E (2018) Prognostic significance of cortactin levels in head and neck squamous cell carcinoma: comparison with epidermal growth factor receptor status. *Br J Cancer* 98, 956–964.
57. Raulf N, Lucarelli P, Thavaraj S, Brown S, Vicencio JM, Sauter T & Tavassoli M (2018) Annexin A1 regulates EGFR activity and alters EGFR-containing tumour-derived exosomes in head and neck cancers. *Eur J Cancer* 102, 52-68.
58. Berns K, Sonnenblick A, Gennissen A, Brohée S, Hijmans EM, Evers B, Fumagalli D, Desmedt C, Loibl S, Denkert C, Neven P, Guo W, Zhang F, Knijnenburg TA, Bosse T, van der Heijden MS, Hindriksen S, Nijkamp W, Wessels LF, Joensuu H, Mills GB, Beijersbergen RL, Sotiriou C & Bernards R (2016) Loss of ARID1A activates AnxA1, which serves as a predictive biomarker for trastuzumab resistance. *Clin Cancer Res* 22, 5238-5248.

59. Gibbs LD, Chaudhary P, Mansheim K, Hare RJ, Mantsch RA & Vishwanatha JK (2018) AnxA2 expression in African American triple-negative breast cancer. *Breast Cancer Res Treat* 174, 113-120.
60. Zhang Y, Bi J, Zhu H, Shi M & Zeng X (2018) AnxA2 could act as a moderator of EGFR-directed therapy resistance in triple negative breast cancer. *Biosci Biotechnol Biochem* 82, 1733-1741.
61. Shetty PK, Thamake SI, Biswas S, Johansson SL & Vishwanatha JK (2012) Reciprocal regulation of annexin A2 and EGFR with Her-2 in Her-2 negative and Herceptin-resistant breast cancer. *PLoS One* 7, e44299.
62. Yi Y, Zeng S, Wang Z, Wu M, Ma Y, Ye X, Zhang B & Liu H (2018) Cancer-associated fibroblasts promote epithelial-mesenchymal transition and EGFR-TKI resistance of non-small cell lung cancers via HGF/IGF-1/AnxA2 signaling. *Biochim Biophys Acta Mol Basis Dis* 1864, 793-803.
63. Grewal T, Hoque M, Conway JRW, Reverter M, Wahba M, Beevi SS, Timpson P, Enrich C & Rentero C (2017) Annexin A6-a multifunctional scaffold in cell motility. *Cell Adh Migr* 11, 288-304.
64. Reverter M, Rentero C, Garcia-Melero A, Hoque M, Vilà de Muga S, Alvarez-Guaita A, Conway JR, Wood P, Cairns R, Lykopoulou L, Grinberg D, Vilageliu L, Bosch M, Heeren J, Blasi J, Timpson P, Pol A, Tebar F, Murray RZ, Grewal T & Enrich C (2014) Cholesterol regulates syntaxin 6 trafficking at trans-Golgi network endosomal boundaries. *Cell Rep* 7, 883-897.
65. Reverter M, Rentero C, de Muga SV, Alvarez-Guaita A, Mulay V, Cairns R, Wood P, Monastyrskaya K, Pol A, Tebar F, Blasi J, Grewal T & Enrich C (2011) Cholesterol transport from late endosomes to the Golgi regulates t-SNARE trafficking, assembly, and function. *Mol Biol Cell* 22, 4108-4123.
66. Alvarez-Guaita A, Vilà de Muga S, Owen DM, Williamson D, Magenau A, García-Melero A, Reverter M, Hoque M, Cairns R, Cornely R, Tebar F, Grewal T, Gaus K, Ayala-Sanmartín J, Enrich C & Rentero C (2015) Evidence for annexin A6-dependent plasma membrane remodeling of lipid domains. *Br J Pharmacol* 172, 1677-1690.
67. Balbis A & Posner BI (2010) Compartmentalization of EGFR in cellular membranes: role of membrane rafts. *J Cell Biochem* 109, 1103-1108.
68. Irwin ME, Mueller KL, Bohin N, Ge Y & Boerner JL (2011) Lipid raft localization of EGFR alters the response of cancer cells to the EGFR tyrosine kinase inhibitor gefitinib. *J Cell Physiol* 226, 2316-2328.
69. Chen Q, Pan Z, Zhao M, Wang Q, Qiao C, Miao L & Ding X (2018) High cholesterol in lipid rafts reduces the sensivity to EGFR-TKI therapy in non-small cell lung cancer. *J Cell Physiol* 233, 6722-6732.
70. Widatalla SE, Korolkova OY, Whalen DS, Goodwin JS, Williams KP, Ochieng J & Sakwe AM (2018) Lapatinib induced Annexin A6 up-regulation as an adaptive response of triple negative breast cancer cells to EGFR tyrosine kinase inhibitors. *Carcinogenesis* 2018 Dec 27. doi: 10.1093/carcin/bgy192.
71. Leca J, Martinez S, Lac S, Nigri J, Secq V, Rubis M, Bressy C, Sergé A, Lavaut MN, Dusetti N, Loncle C, Roques J, Pietrasz D, Bousquet C, Garcia S, Granjeaud S, Ouaissi M, Bachet JB, Brun C, Iovanna JL, Zimmermann P, Vasseur S & Tomasini R (2016) Cancer-associated fibroblast-derived annexin A6+ extracellular vesicles support pancreatic cancer aggressiveness. *J Clin Invest* 126, 4140-4156.

72. Keklikoglou I, Cianciaruso C, Güç E, Squadrito ML, Spring LM, Tazzyman S, Lambein L, Poissonnier A, Ferraro GB, Baer C, Cassará A, Guichard A, Iruela-Arispe ML, Lewis CE, Coussens LM, Bardia A, Jain RK, Pollard JW & De Palma M (2019) Chemotherapy elicits pro-metastatic extracellular vesicles in breast cancer models. *Nat Cell Biol* 21, 190-202.
73. Quattrocelli M, Barefield DY, Warner JL, Vo AH, Hadhazy M, Earley JU, Demonbreun AR & McNally EM (2017) Intermittent glucocorticoid steroid dosing enhances muscle repair without eliciting muscle atrophy. *J Clin Invest* 127, 2418-2432.
74. O'Sullivan D, Dowling P, Joyce H, McAuley E, McCann A, Henry M, McGovern B, Barham P, Kelleher FC, Murphy J, Kennedy S, Swan N, Moriarty M, Clynes M & Larkin A (2017) A novel inhibitory anti-invasive Mab isolated from phenotypic screening highlights AnxA6 as a functionally relevant target protein in pancreatic cancer. *Br J Cancer* 117, 1326-1335.
75. Grewal T, Heeren J, Mewawala D, Schnitgerhans T, Wendt D, Salomon G, Enrich C, Beisiegel U & Jäckle S (2000) Annexin VI stimulates endocytosis and is involved in the trafficking of LDL to the prelysosomal compartment. *J Biol Chem* 275*,* 33806–33813.
76. de Diego I, Schwartz F, Siegfried H, Dauterstedt P, Heeren J, Beisiegel U, Enrich C & Grewal T (2002) Cholesterol modulates the membrane binding and intracellular distribution of annexin 6. *J Biol Chem* 277, 32187-32194.
77. Swarbrick A, Roy E, Allen T & Bishop JM (2008) Id1 cooperates with oncogenic Ras to induce metastatic mammary carcinoma by subversion of the cellular senescence response. *Proc Natl Acad Sci U S A* 105, 5402-5407.
78. Zhou Q, Phoa AF, Abbassi RH, Hoque M, Reekie TA, Font JS, Ryan RM, Stringer BW, Day BW, Johns TG, Munoz L & Kassiou M (2017) Structural optimization and pharmacological evaluation of inhibitors targeting dual-specificity tyrosine phosphorylation-regulated kinases (DYRK) and CDC-like kinases (CLK) in glioblastoma. *J Med Chem* 60, 2052-2070.
79. Friedrich J, Seidel C, Ebner R & Kunz-Schughart LA (2009) Spheroid-based drug screen: considerations and practical approach. *Nat Protoc* 4, 309-324.

Figure legends

Figure 1: AnxA6-induced and PKCα-mediated T654-EGFR phosphorylation inhibits EGFR tyrosine phosphorylation**. (A-B)** Cell lysates from A431wt (lane 1-2) and A431-A6 cells (lane 3-4) incubated ± EGF (10 ng/ml for 3 min) were analyzed for EGFR tyrosine (pY-EGFR) and threonine 654 phosphorylation (pT654-EGFR), total EGFR, AnxA6, PKCα and ß-actin by western blotting as indicated. **(C)** A431-A6 cells were pre-incubated with or without 500 nM TPA overnight to deplete PKC. Cells were serum starved and incubated ± EGF (10 ng/ml for 3 min) as indicated. Cell lysates were prepared and analyzed for EGFR tyrosine phosphorylation (pY-EGFR), total EGFR, PKCα and ß-actin by western blotting. **(D)** A431-A6 cells with stable PKCα knockdown were serum starved and then incubated ± EGF (10 ng/ml for 3 min) as indicated (lane 3-4). A431-A6 cells stably expressing scrambled shRNA served as control (lane 1-2). Cell lysates were prepared and analyzed for pT654-EGFR, total EGFR, PKCα, activated (P-Erk1/2) and total Erk1/2 and ß-actin by western blotting.

Figure 2: AnxA6 reduces A431 tumor growth and EGFR tyrosine phosphorylation *in vivo.* **(A)** The mean tumor mass of xenografts from A431wt and A431-A6 cells ± stable PKCα knockdown was determined as indicated. The mean ± SEM is given (n = 5 per group; * $p < 0.05$, ** = $p < 0.01$, Student's *t*-test). A representative western blot shows PKCα and AnxA6 levels in A431wt and A431-A6 stably transfected with control shRNA (scramble) or shRNA targeting PKCα. **(B-C)** Extracts from A431wt and A431-A6 xenografts ± stable PKCα knockdown (n = 5 per group as indicated) were analyzed by western blotting for EGFR threonine 654 (pT654-EGFR) and tyrosine phosphorylation (pY-EGFR), total EGFR, activated (p-Akt, pS473-Akt) and total Akt, activated (p-Erk1/2) and total Erk1/2. Relative levels of phosphorylated EGFR, Akt and Erk1/2 were normalized to total EGFR, Akt and Erk1/2, respectively. The mean values ± SEM relative to the control (A431wt, scramble) is given (* $p < 0.05$, ** $p < 0.01$, *** $p < 0.001$, **** $p < 0.0001$, Student's *t*-test).

Figure 3: AnxA6 overexpression increases growth inhibition mediated by TKIs targeting EGFR. **(A)** 5 – 8 x 10^3 A431wt (white bars) and A431-A6 (blue bars) were seeded on 96-well plates and grown for 72 h in 10 % FCS with and without 10 µM gefitinib, erlotinib and tyrophostin (AG1478) as indicated. Cell viability in the different treatment groups was compared to the negative control and monitored by MTS assays. Mean values ± SEM of growth inhibition (%)

from 3-4 independent experiments with triplicates samples are given (* $p < 0.05$, Student's *t*-test). **(B)** A431wt and A431-A6 cells ± stable PKCα knockdown were grown ± 5 µM gefitinib as indicated. DMSO served as negative control and growth inhibition (%) in MTS assays was determined as described above. Mean values ± SEM from 3 independent experiments with triplicates samples are given. **(C-D)** For colony forming assays, A431wt and A431-A6 cells were plated in 6-well plates (5 - 7 x 10^3/well) and treated ± 0 - 25 µM erlotinib (C) or 0 - 25 µM gefitinib (D) for five days as indicated. Cells were fixed and stained as described in Material and Methods. Representative images from 3 independent biological experiments with triplicate samples for each condition are shown. Colonies containing more than 20 cells were quantified using ImageJ software. The number of colonies ± SD is given (*** $p < 0.001$, Student's *t*-test).

Figure 4: AnxA6 expression in A431 squamous carcinoma cells reduces EGF-inducible cell migration. **(A-B)** A431wt and A431-A6 cells stably expressing scrambled shRNA or shRNA targeting PKCα were seeded in 6-well plates, grown until 90 % confluency in 10 % FCS and then wound healing assays were performed as described in Material and Methods. Representative images at t = 0 h and t = 12 h are shown. The relative wound density (RWD %) at 12 h and 24 h from 3 independent experiments with triplicate samples was calculated using ImageJ (* $p < 0.05$, ** $p < 0.01$, **** $p < 0.001$, Student's *t*-test). **(C-D)** A431wt and A431-A6 cells were grown until 90 % confluency, starved overnight and then wound healing assays ± EGF (10 ng/ml) were performed as described above. Representative images from t = 0 h and t = 12 h are shown. The RWD (%) at t = 6 h and t = 12 h from 3 independent experiments with triplicate samples was calculated (* $p < 0.05$, *** $p < 0.001$, Student's *t*-test).

Figure 5: Reduced migration of AnxA6 expressing A431 squamous carcinoma cells improves TKI efficacy. **(A-B)** A431wt and A431-A6 cells were seeded in 6-well plates, grown until 90 % confluency and then wound healing assays were performed ± erlotinib (2 - 5 µM) and ± gefitinib (2 - 5 µM) as indicated. Representative images at t = 0 h and t = 12 h from cells incubated ± 5 µM EGFR-TKIs are shown. The relative wound density (RWD %) at 12 h from 3 independent experiments with triplicate samples was calculated using ImageJ. The mean values ± SEM are given (* $p < 0.05$, ** $p < 0.01$, Student's *t*-test).

Figure 6: Reduced invasion of AnxA6 expressing A431 squamous carcinoma cells improves TKI efficacy. A431wt and A431-A6 cells (2 x 10^3 cells/well) were seeded in 96-well plates and after 24 h, each well was scratched using the WoundMaker (IncuCyte). **(A-B)** Cells were treated ± 1 µM erlotinib or gefitinib and cell migration after 24 h was quantified. **(C-D)** MatriGel Matrix was added to each well and once the Matrigel Matrix was set, cells were treated ± 1 µM erlotinib or gefitinib and invasion after 72 h was quantified. Representative images at t = 0, 24 (A) and 72 h (C) are shown. The relative migration (%) in (B) and relative invasion (%) in (D) from 3 independent experiments with triplicate samples was calculated using ImageJ. The mean values ± SEM are given (* $p < 0.05$, ** $p < 0.01$, *** $p < 0.001$, Student's *t*-test).

Figure 7: AnxA6 expressing A431 squamous carcinoma cells show improved TKI efficacy in 3D spheroids. **(A)** A431wt and A431-A6 cells were plated on agarose-coated 96-well plates. After 2 days, cells were incubated with 0 - 10 µM gefitinib or erlotinib for additional 7 or 22 days as indicated. **(B-C)** The relative spheroid growth after 7 and 22 days (B) and invasion ('sprouting') after 22 days (C) from 3 independent experiments with triplicate samples was calculated using ImageJ (* $p < 0.05$, Student's *t*-test).

Graphical abstract

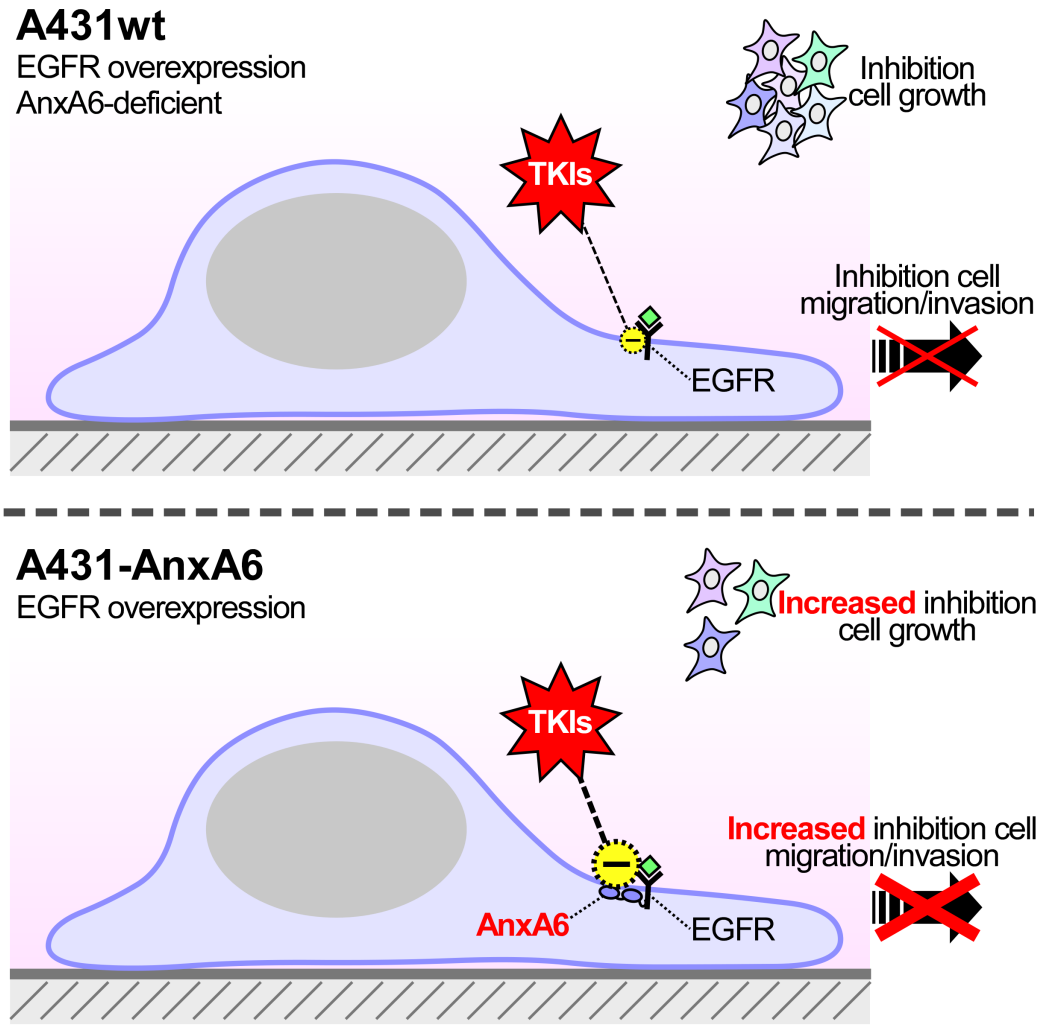

Figure 1

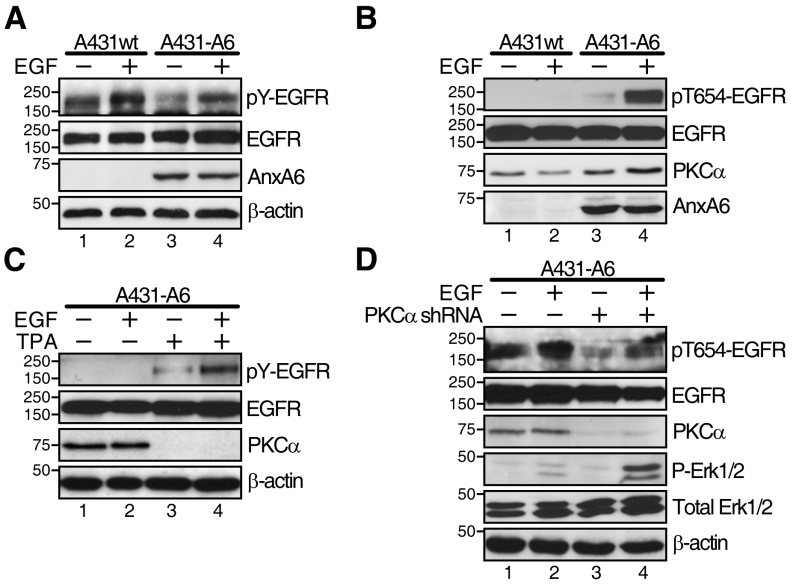

Figure 2

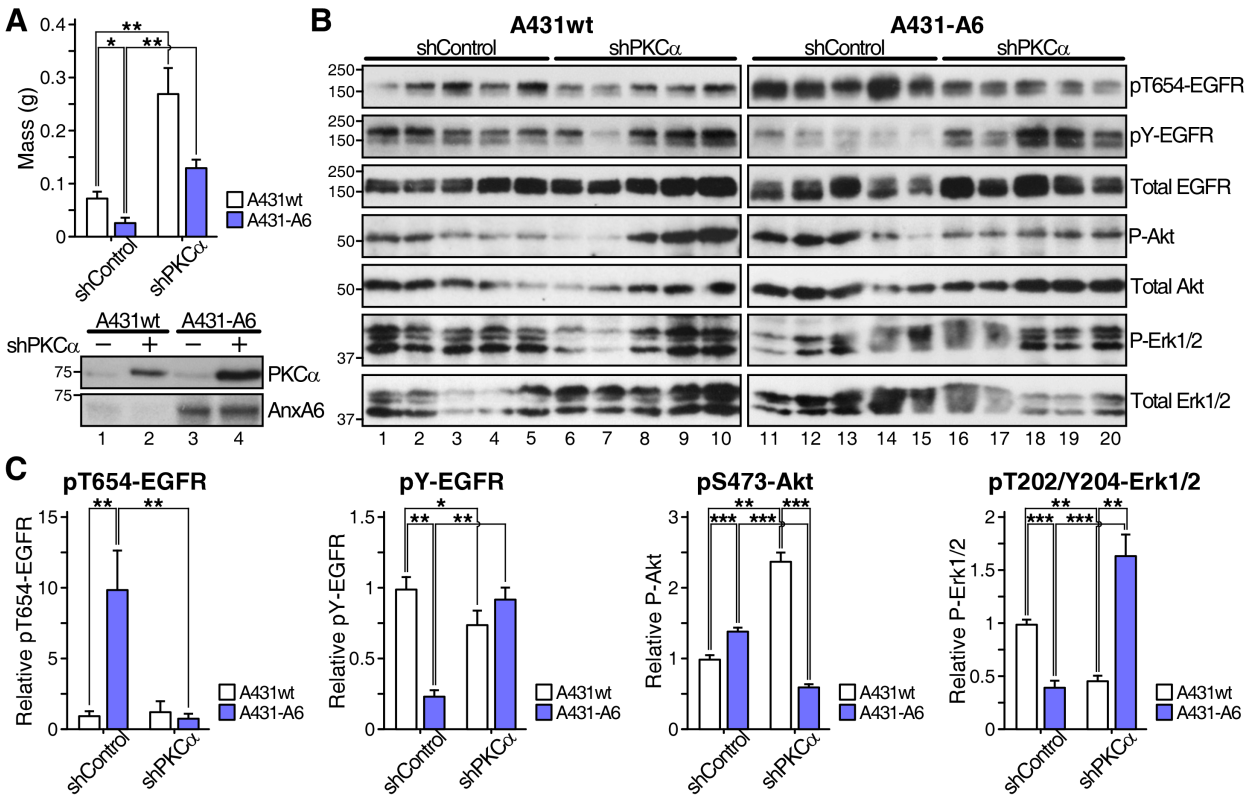

Figure 3

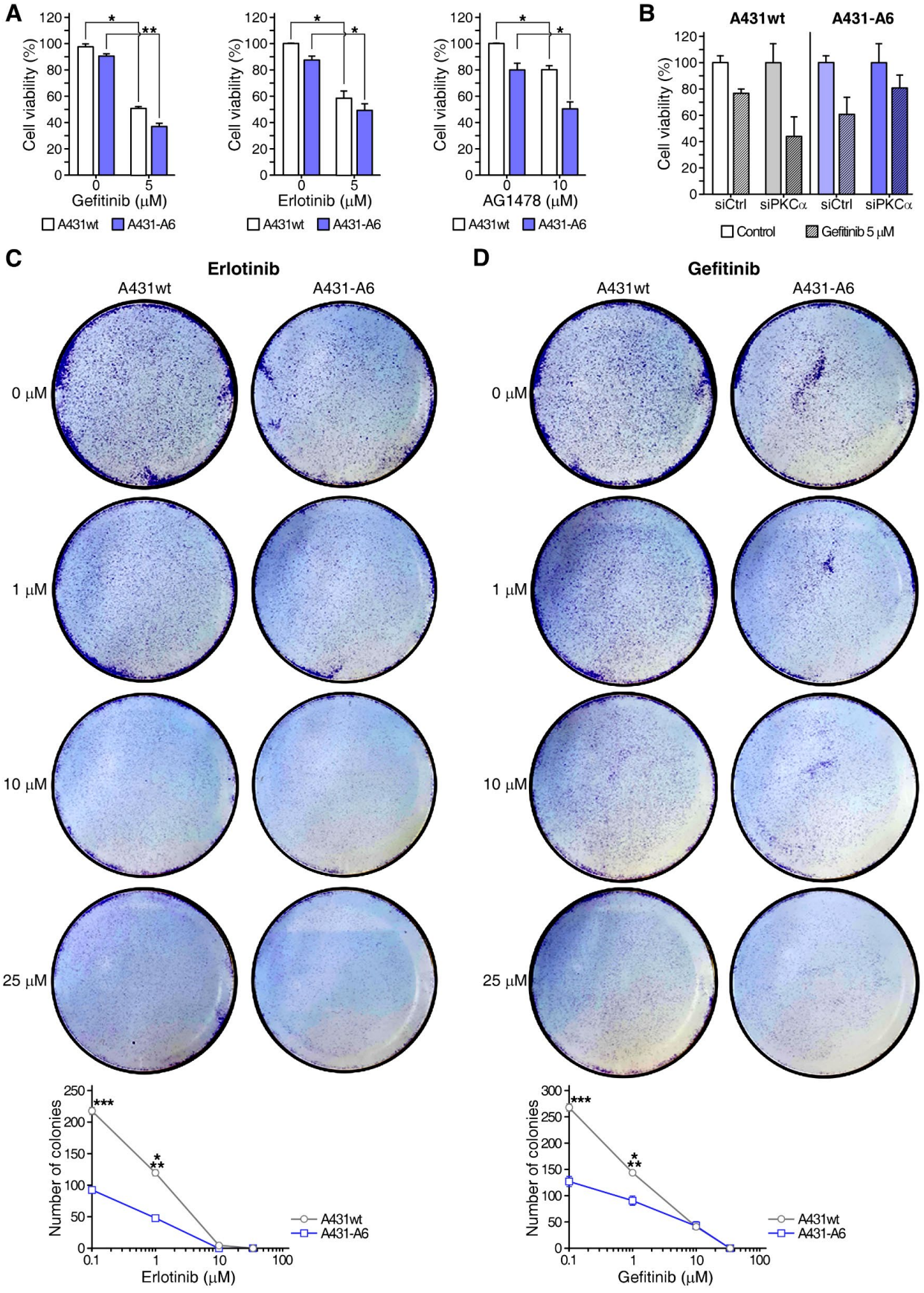
A
Cell viability (%)
Gefitinib (μM)
Erlotinib (μM)
AG1478 (μM)
A431wt
A431-A6
B
A431wt
A431-A6
siCtrl
siPKCα
Control
Gefitinib 5 μM
C
Erlotinib
D
Gefitinib
0 μM
1 μM
10 μM
25 μM
Number of colonies

Figure 4

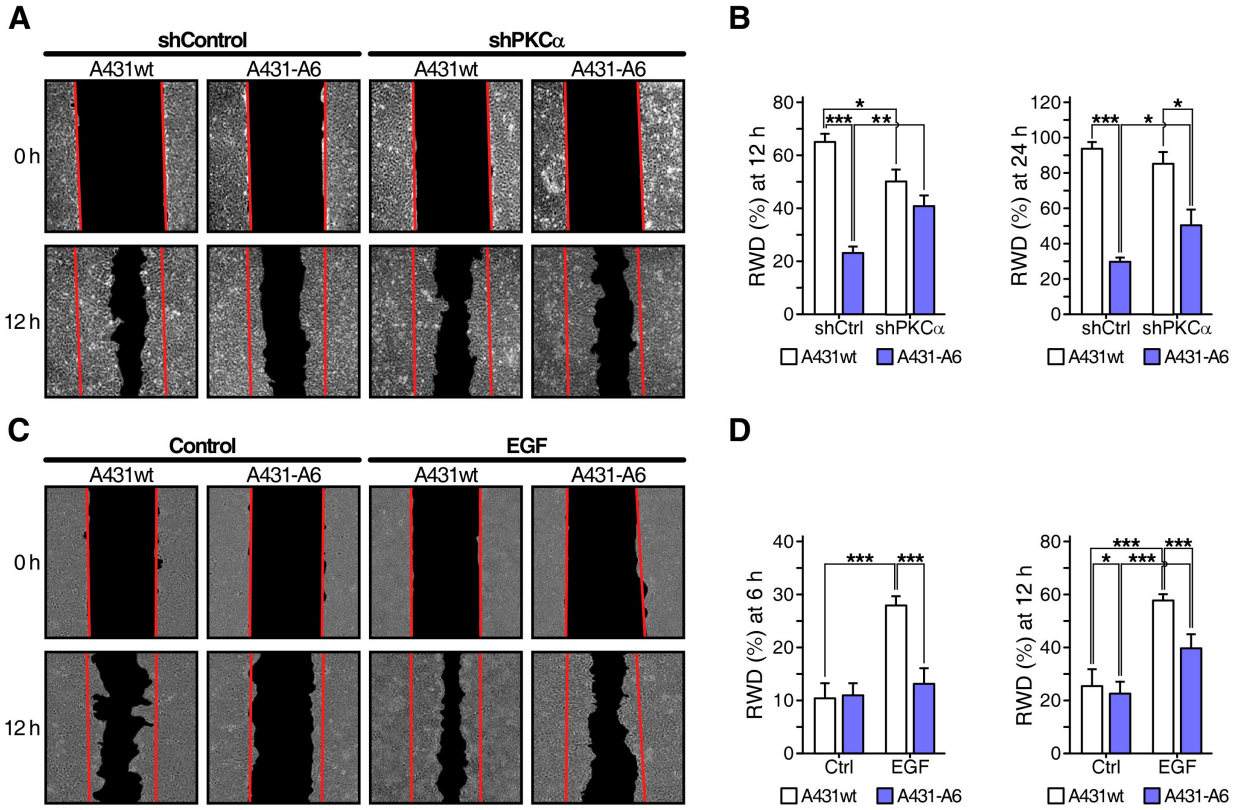

Figure 5

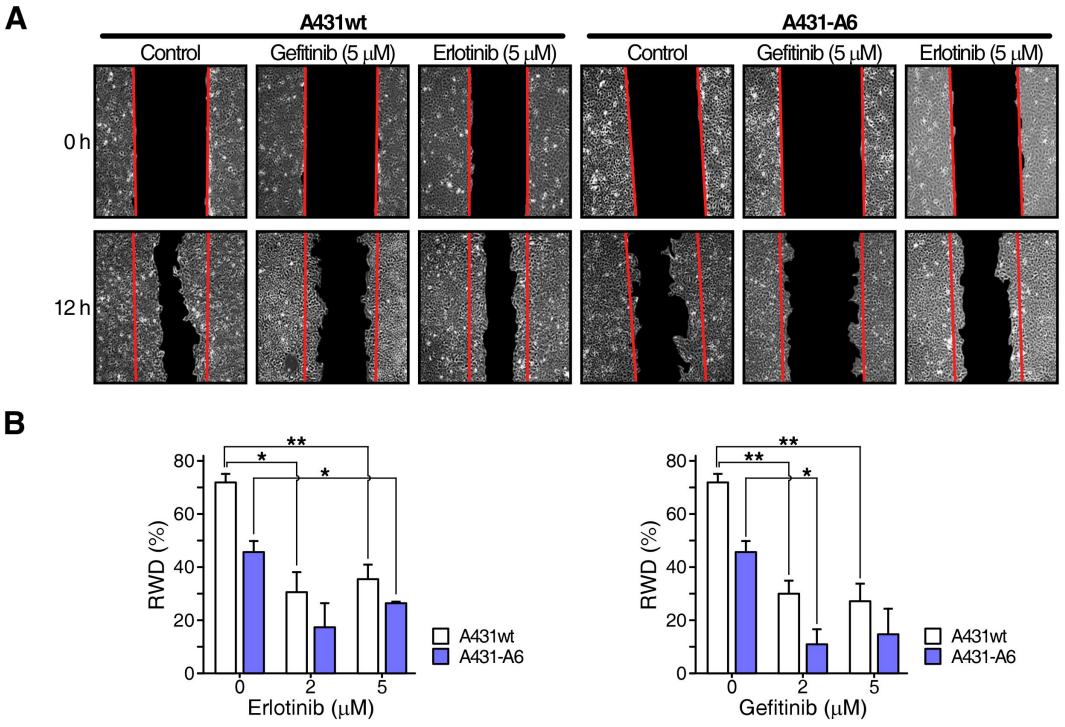

Figure 6

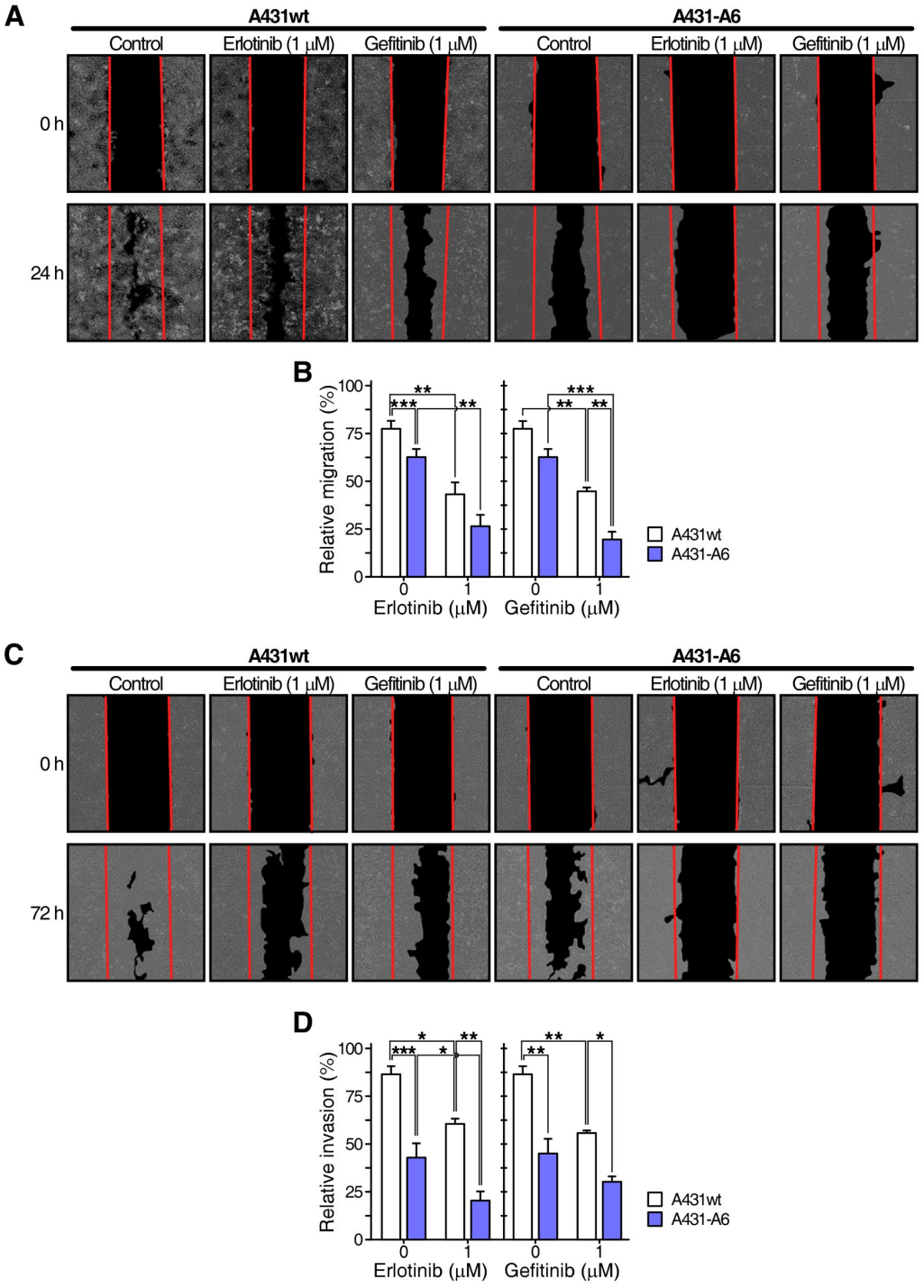
A
A431wt
A431-A6
Control
Erlotinib (1 μM)
Gefitinib (1 μM)
Control
Erlotinib (1 μM)
Gefitinib (1 μM)
0 h
24 h
B
Relative migration (%)
100
75
50
25
0
**
***
**
***
**
**
***
**
**
0
1
0
1
Erlotinib (μM)
Gefitinib (μM)
A431wt
A431-A6
C
A431wt
A431-A6
Control
Erlotinib (1 μM)
Gefitinib (1 μM)
Control
Erlotinib (1 μM)
Gefitinib (1 μM)
0 h
72 h
D
Relative invasion (%)
100
75
50
25
0
*
***
*
**
**
**
*
**
0
1
0
1
Erlotinib (μM)
Gefitinib (μM)
A431wt
A431-A6

Figure 7

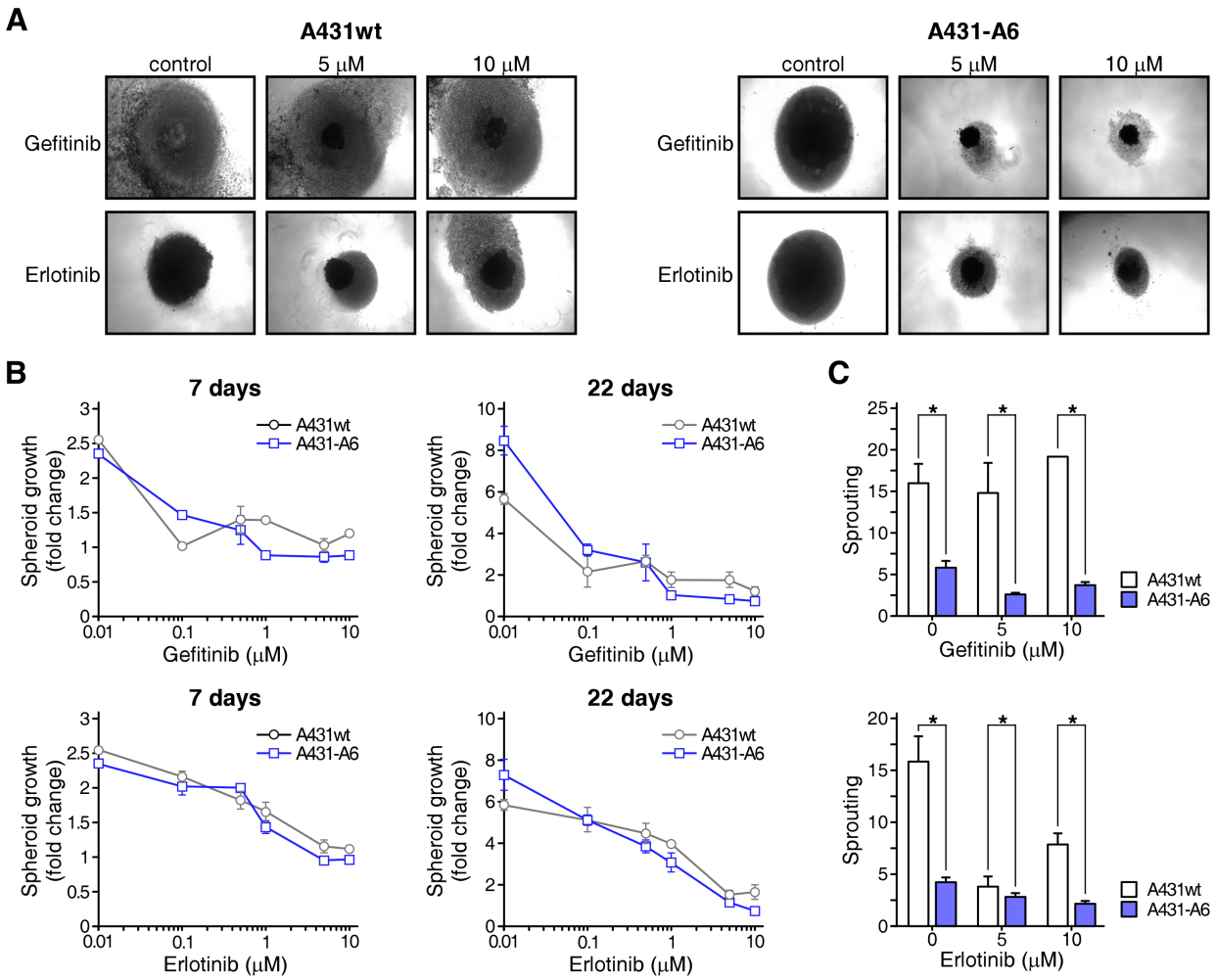
A
A431wt
A431-A6
control
5 μM
10 μM
Gefitinib
Erlotinib
B
7 days
22 days
Spheroid growth (fold change)
A431wt
A431-A6
Gefitinib (μM)
Erlotinib (μM)
C
Sprouting
Gefitinib (μM)
Erlotinib (μM)